A Geometric Determination of Void Production in an Elastic Pancake

PAUL J. BLATZ and P. KAKAVAS*,†

Blatz Institute of Rubber Elasticity, 5825 Norwich, Van Nuys, California 91411

SYNOPSIS

The aim of this article is to adduce various theoretical approaches to evaluating the stress displacement field throughout a pancake sample. We shall attempt to produce an effective material property, ν_{eff}, which is consistent with the measured values of $\gamma = -u_0(a)/a\varepsilon$ (normalized volumetric contraction), the initial modulus from the triaxial tests on compression, M_{compr}, and tension, M_{tens}. In order to obtain analytical expressions relating γ and $(M/E)_{\text{tens}}$ to ν_{eff}, we used the simplest finite element mesh. Taking the given aspect ratio of the pancake $\left(\frac{D}{h} \approx 16\right)$, the shear modulus $G = 60$ psi, and the measured $\gamma = 0.23$, it was found that the effective Poisson's ratio is $\nu_{\text{eff}} \approx 0.492$ and the initial modulus in tension $M_{\text{tens}} = 2990$ psi. Using Warren's equation, one obtains the volume fraction of voids from the determined effective material property ν_{eff}. It was found that the volume fraction of voids α grows from 0.002 to 0.021. © 1993 John Wiley & Sons, Inc.

INTRODUCTION

The motivation for writing this article is based on the belief that unfilled elastomers, in general, are "slightly" porous. This article will attempt to define, by both geometric and mechanical measurements, what is meant by the term "slightly." This belief arises from these observations:

1. If one plots the measured values of volume contraction, produced by hydrostatic pressure (Fig. 1[1]), one observes an initial rapid contraction, corresponding to the early collapse of voids. Much attention has been given to this phenomenon. Articles by Blatz,[2] Milloway,[3] and Herrmann[4] all lead to analytical expressions from which one can calculate two parameters: void volume fraction and shear modulus, which are consistent with the initial curvature and limiting slope, displayed in Figure 1.
2. If one plots simple tension data in the form $\frac{\sigma}{\lambda - 1/\lambda^2}$ vs. $\frac{1}{\lambda}$, where σ is the Piola stress and λ the stretch ratio, one observes again an early rapid drop in Young's modulus (Fig. 2[5,7]), which again we ascribe to void collapse.
3. Both simple tension data[6] and triaxial–pancake data,[7] obtained quasistatically ($\dot{\varepsilon} \to 0$), evince hysteresis between load and unload in any one loading cycle. Since viscoelasticity dissipation is negligible at low rates of extension, and in a temperature range at least 100°C above the glass transition temperature, we again ascribe the hysteresis to a mechanical difference between void opening and void closing. Figure 3 shows the Young's modulus vs. strain rate for our nitrile rubber, with $T_g = -80$°C, at ambient temperature (20°C). Figure 3 confirms the statement that our rubber is essentially nonviscoelastic.

Because of our knowledge and familiarity with these observations, we set out to provide a direct measurement of volume change in a stress field, which enhances the void opening and void growth. We prepared a supply of pancake-shaped specimens

* Present address: ASPA PLAST SA., 135 Korinthou Street, 262-23 Patras, Greece.

† To whom correspondence should be addressed.

Journal of Applied Polymer Science, Vol. 49, 2197–2205 (1993)

CCC 0021-8995/93/122197-09

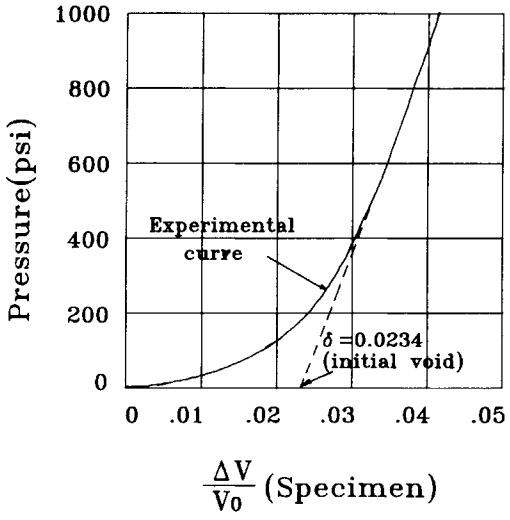

Figure 1 Effect of shear modulus fitting PV data for a voided composite material.[1]

of acrylanitrile–butadiene acid copolymeric elastomers (Table I). These specimens were designed to have a thickness of 0.381 in. and a radius of 3.0 in. Such a specimen, whose thickness/diameter ratio is 1/16 of a barrel unit, is called a pancake (Fig. 4). The specimens were all bonded with Chemlok 205 adhesive to steel plates, thick enough to be considered rigid. Such sandwich combinations were then subjected to cyclical loading to various strain levels

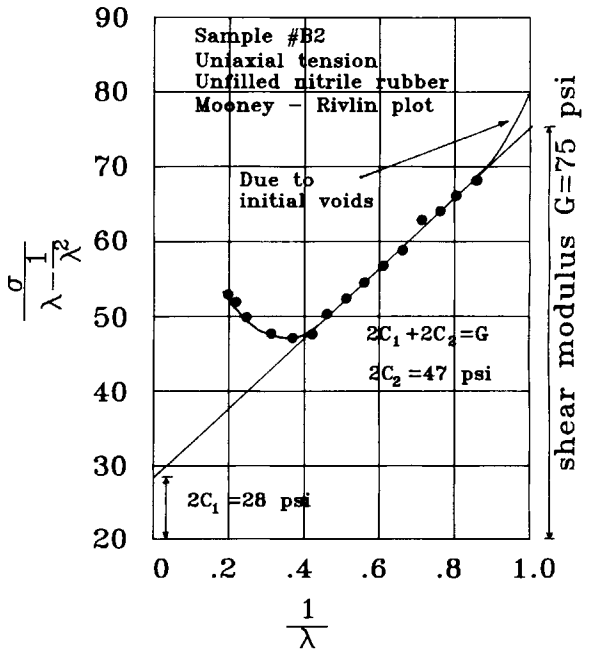

Figure 2 The uniaxial deformation of natural rubber fitted to transversely isotropic Mooney–Rivlin strain energy function.[5]

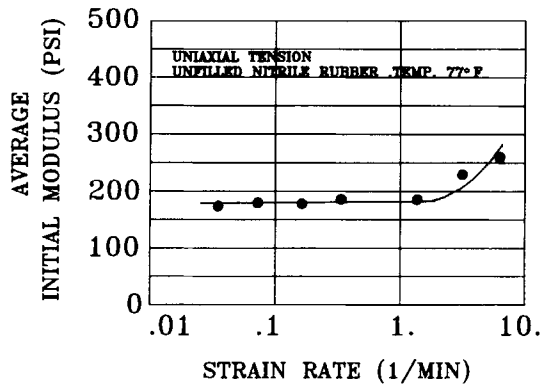

Figure 3 Initial modulus E vs. strain rate $\dot{\varepsilon}$ for our unfilled nitrile rubber whose chemical composition is presented in Table I.

in both tension and compression, provided by an MTS testing machine. All displacements rates, both in loading and in unloading, were fixed at 0.01 in./min, which corresponds to $\dot{\varepsilon} = 0.267\ \text{min}^{-1}$. A typical set of loading curves is shown in Figure 5.

While stretching slowly from 0 to 25% strain, we measured the diametral contraction of the midplane. Figure 6 shows the experimental values of $-u_0(a)/a$, plotted vs. ε, where α is the radius of the pancake (≈ 3 in.) and $-u_0(a)$ is the radial contraction of the midplane ($z = 0$), measured at the edge ($r = a$). The best numerical value of the slope γ, based on a linear regression estimate, is 0.23.

If we denote the effective pancake modulus by M, we then have the two best values (Fig. 7):

$$M_{\text{compr}} = 6100 \text{ psi}$$

$$M_{\text{tens}} = 2500\text{–}2700 \text{ psi}$$

What we proposed to do in the next section was to adduce various theoretical approaches to evaluating

Table I Chemical Composition of the Unfilled Nitrile Rubber Samples

Chemical Composition	Parts (gms)	Density (ρ_i)	Vol. Fractions (ν_i)
NBR (KRYNAC-800)	100.0	1.06	0.949821
Zinc oxide	5.0	5.47	0.009203
Stearic acid	1.0	0.847	0.011887
N-Isopropyl-*N*-Phenyl-*P*-Phenyllenediamine	1.0	1.3	0.00745
Magnesium carbonate treated elemental sulfur	2.0	2.07	0.009728
Benzothiazyl disulfide	1.5	1.3	0.011617

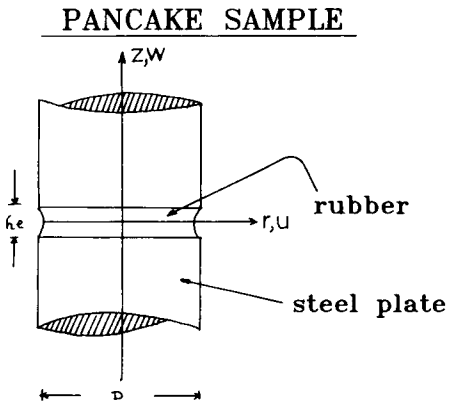

Figure 4 Pancake testing sample and the coordinate system used in the stress analysis.

the stress–displacement field throughout the pancake. Then we attempted to produce an effective material property (ν_{eff}), which, in turn, is consistent with the measured values of (γ, M_{compr}, M_{tens}).

The limitations of this experimental work are as follows:

An "unfilled" rubber is "slightly" porous. Our particular nitrile rubber contains 2% by wt ZnO, with a density of 5.47. This corresponds to a content of rigid filler particles *ca.* 0.9% by volume. The meaning of "unfilled" is anything less than 1%. It probably is possible to prepare samples with 0% filler particles, using DiCup cure, as did Wood et al.[8] at the N.B.S.

The meaning of "slightly" is approximately 0.01 to 0.1 vol % in the virgin specimen. Thus, we expect the virgin material to evince a rapid collapse of volume in such amount, prior to evincing the stiffness associated with the bulk modulus of *ca.* 1 *M*psi.

Unpublished data, determined by A. Lepie[9] at the N.W.C., China Lake, California, on a number of unfilled rubber polymers evince collapse volumes, such as 2%, matching C. Surland's pioneering work.

When a pancake is first compressed, a number of things should be done, which were not done in this case.

First, an upper limit of compression, for example 5%, should be chosen. Then (always maintaining the loading rate at 0.01 in./min), the pancake should be squeezed to 5%, unloaded to 0%, and checked for any permanent set, which may have arisen from the glue line. Second, the two slopes should be compared for consistency. Third, this cycle should be repeated several times until the best value of M_{compr} is obtained. Fourth, the diametral bulge of the midplane should be measured. If calipers with dull pointed tips are used, (radius of curvature $\equiv$ 400 μ), then $u_0(a)$ can be measured accurately to better than 5%. Finally, the range of compressive strain can be extended from 5% to 10% and the whole procedure can be repeated.

When one passes from compression to tension, two additional features of behavior enter the problem. First, the original 0.02% voids may grow rapidly to approximately 2% for two reasons. The voids in the virgin material are maintained in a semiclosed, buckled state by weak adhesive forces, engendered by the curing process (temperature and pressure). Second, additional voids may arise by virtue of the breaking of weak adhesive bonds between the gum stock and any filter particles, such as zinc oxide. In order to sort out these effects, it is worthwhile to cycle between -5% and 5% strain, doing all the checks suggested above, along with measuring $-u_0(a)$ as well as $+u_0(a)$.

Finally, another phenomenon occurs, namely an ablative type of tearing of the voids, which the data of Figure 5(a) suggest becomes important when the tensile strain exceeds 20%.

In obtaining the data for Figure 5(b), we cycled a sample between 0 and 10% tensile strain. The modulus M_{tens} dropped from 6100 psi in the first pull to 2500 psi in the fourth pull, which stays fairly constant thereafter.

The stress field in the interior of the pancake is essentially hydrostatic, as shown below. Thus, the stress field at the surface of most voids is essentially equibiaxial. In order to document the statement that tear starts at 20% strain, this equibiaxial strain is converted to a biaxial stress at the void surface and that stress is compared with an experimentally measured value of failure stress in equibiaxial loading.

Conversely, after a critical uniaxial strain is identified, below which voids do not tear, then the hysteresis must be ascribed to buckling phenomena.

In performing the type of program discussed above, it is important to realize that all behaviors approach limiting values, such as $(a/h) \rightarrow \infty$. Thus, a systematic experimental program will include measurements made over a range of aspect rations $(2\ a/h)$ = 8, 12, 16, 20, 24, and so on. The upper limit that is experimentally achievable is determined by the available load cell and type of testing machine.

THE STRESS–DISPLACEMENT FIELD

First, the domain of the pancake is geometrized by embedding cylindrical coordinates. Below is a sketch of a one quarter domain with boundary conditions:

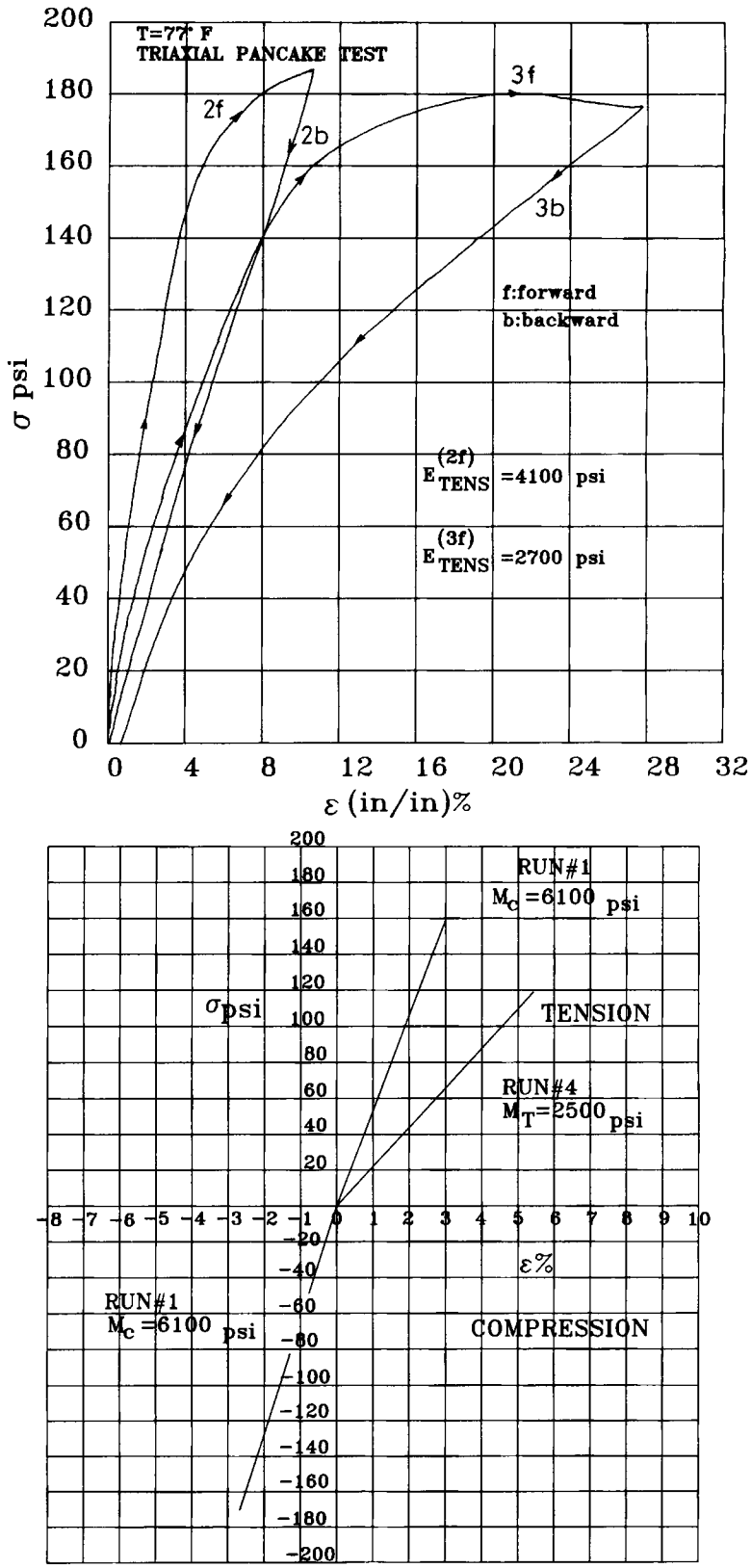

Figure 5 (a) Stress–strain curves with hystersis from a pancake sample, subjected to uniform tension (the chemical composition of the sample is presented in Table I). (b) Stress–strain curves in tension and compression at low values of strain ($2500 \leq M_{tens} \leq 6100$ psi and $M_{comp} \approx 6100$ psi).

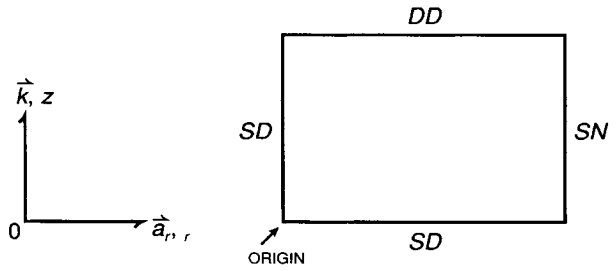

The upper surface is a DD-surface, with two displacements specified at

$$z = \frac{h}{2}\begin{cases} u = 0 \\ w = \varepsilon h/2 \end{cases}$$

The right boundary is an SN-boundary at

$$r = a\begin{cases} \sigma_r = 0 & \text{(normal)} \\ \tau_{rz} = 0 & \text{(shear)} \end{cases}$$

The lower boundary is an SD-surface at

$$z = 0\begin{cases} w = 0 \\ \tau_{rz} = 0 & \text{(shear)} \end{cases}$$

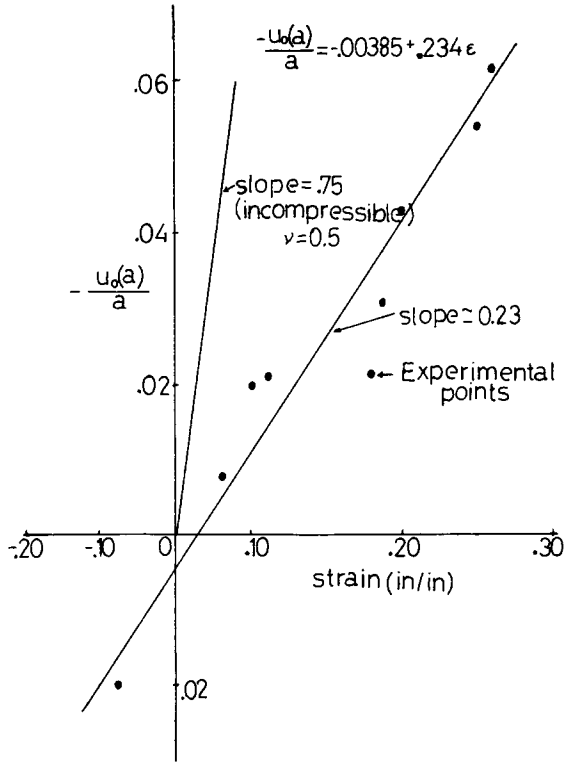

Figure 6 Measured values of the lateral contraction of the mid-plan $-u_0(a)/a$ vs. strain ε for our "unfilled" nitrile rubber pancake samples (aspect ratio $2a/h = 16$).

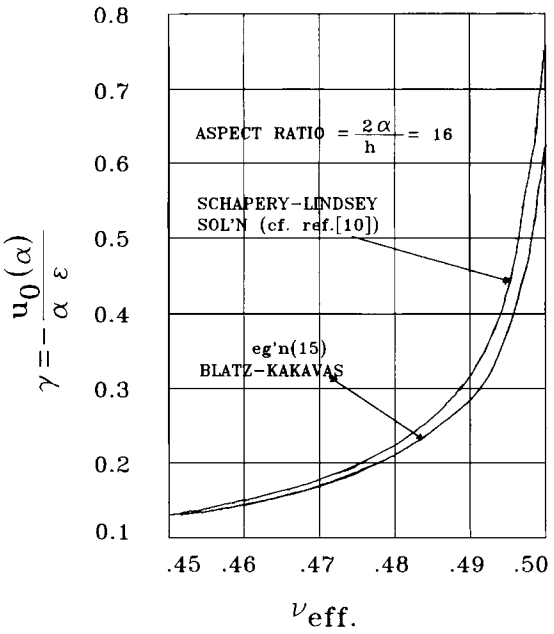

Figure 7 Diametral contraction $\gamma = -u_0(a)/a$ vs. effective Poisson's ratio ν_{eff} from eq. (15), using the IMSL computer subroutines.

and likewise, the left boundary is an SD-surface at

$$r = 0\begin{cases} u = 0 \\ \tau_{rz} = 0 & \text{(shear)} \end{cases}$$

Much work has been performed on this problem. Levinson[10] inputed neo-Hookean character to the rubber, assuming that all z-planes remained parallel to the z-axis and produced a variational solution. About the same time Lindsey et al.[11] used a variational approach with material linearity, and the dual assumptions:

$$w = \varepsilon z \tag{1}$$

$$u = c(r)\left(\frac{4z^2}{h^2} - 1\right) \tag{2}$$

We repeat here the evolution of their solution, obtained by minimizing a Helmholtz potential energy.

From eqs. (1) and (2), one obtains:

$$e_r = u_r = c'(r)\left(\frac{4z^2}{h^2} - 1\right) \quad \text{(radial strain)} \tag{3}$$

$$e_\theta = (u/r) = (c/r)\left(\frac{4z^2}{h^2} - 1\right)$$

(tangential strain) (4)

$$e_z = w_z = \varepsilon \quad \text{(axial strain)} \tag{5}$$

$$e_{rz} = (u_z + w_r)/2 = c(r)(4z/h^2) \quad \text{(shear strain)} \tag{6}$$

$$W = (G/(1-2\nu))[(1-\nu)(e_r^2 + e_\theta^2 + e_z^2) + 2(1-2\nu)e_{rz}^2 + 2\nu(e_r e_\theta + e_r e_z + e_\theta e_z)] \quad \text{(strain energy)} \tag{7}$$

$$\Phi = \int_{-h/2}^{h/2} dz \int_0^a 2\pi r\, dr W \quad \text{(Helmholtz free energy function)} \tag{8}$$

Note that the other term in the function, namely the potential of the external forces, contributes nothing along the SD, SD, and SN boundaries (*cf.* Levinson[10]).

Using calculus of variations, $\delta\Phi = 0$ is set and, after skipping the algebraic details, the following is obtained:

$$u = \left(\frac{4z^2}{h^2} - 1\right)\frac{I_1(\theta)}{I_1(\theta_1)} \cdot \frac{5\nu\varepsilon a}{4[(1-\nu)m - (1-2\nu)]} \tag{9}$$

where

$$\theta = kr/h \tag{10}$$

$$\theta_1 = ka/h \tag{11}$$

$$k = \sqrt{5(1-2\nu)/(1-\nu)} \tag{12}$$

$$m = \theta_1 I_0(\theta_1)/I_1(\theta_1) \tag{13}$$

and

$$(M/E)_{\text{tens}} = \frac{(1-\nu) - \{(5\nu^2)/[3[(1-\nu)m - (1-2\nu)]]\}}{(1-2\nu)(1-\nu)} \tag{14}$$

Lindsey,[11] starting from z-averaged equilibrium equations, rather than from the functional equations, obtained 6 instead of 5 under the radical in the definition of kappa.

M is obtained by setting

$$\Phi_{\min}/\pi a^2 h = M\varepsilon^2/2$$

From eq. (9), we observe that:

$$\gamma \equiv -u_0(a)/a\varepsilon = \frac{5\nu}{4[(1-\nu)m - (1-2\nu)]} \tag{15}$$

Figure 7 shows how ν_{eff} depends on γ_{meas}. With $\gamma_{\text{meas}} = 0.23$ and $(a/h) = 7.87$, $\nu_{\text{eff}} = 0.479$ is obtained. After 0.479 is inserted into eq. (14), with $E = 180$ psi (Fig. 3), $M = 1084$ psi is obtained, which is well below the measured value of approximately 2500–2700 psi. On the contrary, if one reverses the procedure and calculates ν_{eff} from M_{meas}, one obtains 0.492, which predicts that γ_{meas} should be 0.34, 50% higher than that which was measured. We predict that the starting assumptions, eqs. (1) and (2) of the variational analysis, are too crude. Physically, the axial displacement is expected to be a function of the form:

$$w = \varepsilon z + d(r)\left(\frac{h^2 z}{4} - z^3\right)$$

which allows the z-planes to warp at the free surface (see sketch below):

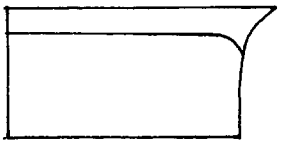

This effect cannot be predicted by a second-order differential equation. One needs the full fourth order theory, which is analytically tedious, in order to obtain the correct z-dependencies for u and w at the edge ($r = a$).

Thus, finite elements were investigated. In order to obtain analytical expressions relating γ and M/E to ν_{eff}, we took the simplest mesh possible, namely:

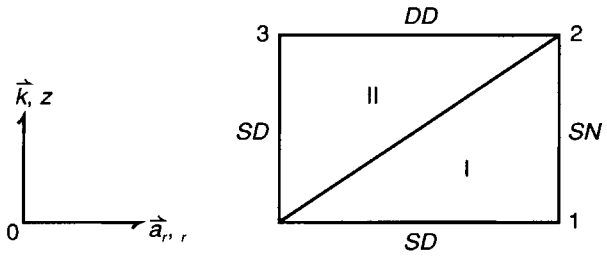

two elements, and one free node (#1).

After choosing shape functions that were linear in r and z, we evaluated the functional, differentiated with respect to u_1, set it equal to zero, and evaluated all desired quantities, much as was done in the I-element process discussed earlier. All the details are provided in the Appendix.

The resulting expressions are:

$$\gamma = \frac{9\nu}{2[(4-\nu) + 6(1-2\nu)(a/h)^2]} \tag{16}$$

$$M = \frac{(2-2\nu)}{(1-2\nu)} G\left(1 - \frac{\nu}{1-\nu}\gamma\right) \tag{17}$$

with $(a/h) = 8$, $G = 60$ psi, $\gamma = 0.23$, one obtains $\nu_{\text{eff}} = 0.492$ and $M = 2990$ psi.

These results bring the measured γ in line with the measured M. What remains to be done is to refine the mesh and, using a good axisymmetric finite element code, to find the values of γ and M as functions of the parameters ν_{eff} and a/h. We are in the process of doing this. Pickett[12] and Brady[13] have addressed this problem. The published curves do not, however, apply to our aspect ratio ($2\ a/h = 16$). We hope that this work will inspire other investigators to produce diametral mid-plane deformations of pancakes, as well as to inspire other computer experts to provide accurate numerical evaluations of the pancake stress–displacement field for an appropriate range of aspect ratios.

VOIDS

With the measured values $\gamma = 0.23$, $M_{\text{tens}} = 2500$ psi in hand, and a linear finite element method (FEM) calculation (albeit crude), producing an effective Poisson's ratio, $\nu_{\text{eff}} = 0.492$, it is tempting to ask what volume fraction of voids corresponds to this ν_{eff}.

An immediate answer is provided by Warren,[14] who, on the basis of linear analysis, arrives at

$$\alpha = \frac{2-4\nu}{3-3\nu} \rightarrow \begin{cases} \nu \cong 1/2 \rightarrow 0 \\ \nu \cong -1 \rightarrow 1 \end{cases} \tag{17}$$

with $\nu = 0.492$ and $\alpha = 0.021$ (α is the volume fraction of voids).

Thus, we conclude that, as we cycle from 0–10% tensile strain

M_{tens} falls from 6100 to 2500 psi
ν falls from 0.49994 to 0.492
α grows from 0.002 to 0.021

Note that $(1 - (E/3K))/2 = 0.49994$, $E = 180$ psi (measured), and $K = 500{,}000$ psi (measured).

A more exacting answer is provided by the nonlinear theory. We first stretched some O-rings, made from the same material, in simple tension at the same rate and temperature. A typical curve is shown in Figure 8.

We chose a 1-term Ogden strain energy of the form[15]:

$$W = \frac{2G}{n}\sum_{\alpha}\left[\frac{(\lambda_\alpha^n - 1)}{n} - \ln(\lambda_\alpha)\right] - p\ln(J), \qquad J = 1 \tag{18}$$

The Cauchy stress principle is given by:

$$t_\alpha = \sigma_\alpha\lambda_\alpha = \lambda_\alpha\frac{\partial W}{\partial\lambda_\alpha} = 2G\left(\frac{\lambda_\alpha^n - 1}{n}\right) - p \tag{19}$$

where σ_α is the Piola stress principle.
In simple tension, eq. (19) is reduced to:

$$\sigma = \frac{2G}{n}(\lambda^{n/2} - \lambda^{-n/2}) \tag{20}$$

An excellent fit up to 300% strain is obtained with $G = 60$ psi ($=E/3$) and $n = 1.6$.

The next step is to solve the problem of pressurizing a thick spherical shell, $A \le R \le B$. The void (radius A) is traction-free and to the outer surface ($R \ge B$) is applied pressure P. For this geometry, $\lambda_1 = 1/\lambda^2$ and $\lambda_2 = \lambda_3 = \lambda$.

Skipping algebraic details, one obtains:

$$t_1 = \sigma_1\lambda_1 = \frac{2G}{n}\left\{\frac{\lambda^{-2n} - \lambda_b^{-2n}}{n} - 2\int_{\lambda_b}\left(\frac{\lambda^{3n} - \lambda^3}{\lambda^3 - 1}\right)\frac{d\lambda}{\lambda^{2n+1}}\right\} - P \tag{21}$$

$$t_2 = \sigma_2\lambda_2 = \frac{2G}{n}\left\{\lambda^n - \frac{\lambda_b^{-2n}}{n} - \frac{(n-1)\lambda^{-2n}}{n} - 2\int_{\lambda_b}\frac{(\lambda^{3n} - \lambda^3)}{(\lambda^3 - 1)}\frac{d\lambda}{\lambda^{2n+1}}\right\} - P \tag{22}$$

at $R = A$, $t_1 = 0$, thus,

$$\frac{Pn}{2G} = \lambda_\alpha^{-2n} - \lambda_b^{-2n} + 2\int_{\lambda_\alpha}^{\lambda_b}\left(\frac{\lambda^3 - \lambda^{3n}}{1 - \lambda^3}\right)\frac{d\lambda}{\lambda^{2n+1}} \tag{23}$$

which, after suitable approximation, leads to:

$$\lambda_a^3 = \left(1 + \frac{nP}{2G}\right)^{-3/2n} \tag{24}$$

$$\lambda_b^3 = \alpha\left(1 + \frac{nP}{2G}\right)^{-3/2n} + (1 - \alpha);\ \alpha = (A/B)^3 \tag{25}$$

$$T = (\sigma_2\lambda_2)_a = \frac{2G}{n}(\lambda_a^n - \lambda_\alpha^{-2n}) \tag{26}$$

as

$$-\frac{2G}{n} < P < \infty$$
$$\infty > \lambda_a^3 > 0 \quad \text{(void closure)}$$
$$\infty > \lambda_b^3 > (1 - \alpha)$$
$$\infty > T > -\infty \tag{27}$$

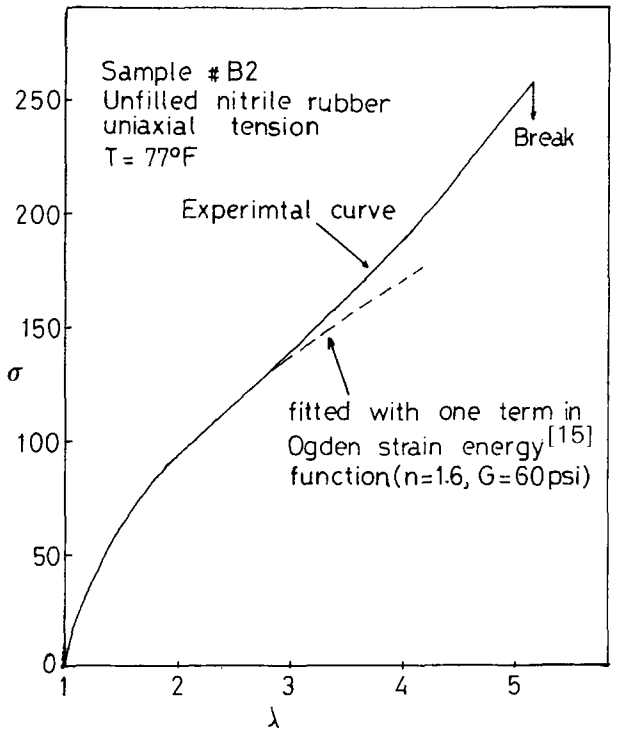

Figure 8 Stress–strain data from O-ring samples using unfilled nitrile rubber (Table I). The data were fitting with one-term Ogden energy function.

When P becomes negative, λ_a^3 rises rapidly; all rubbers, following the notation of Prager, are "locking" materials, and start to fail when λ reaches λ_{max} = 6. With λ_{max} = 6, G = 60 psi, n = 1.6, and α = 0.021, T_{max} = 1320 psi is obtained, which should match the measured equibiaxial failure stress.

It is hoped that other investigators pursue this checkpoint. The spherical shell solution, evaluated at $R = B$, is essentially hydrostatic

$$(\sigma_1\lambda_1)_{R=B} = (\sigma_2\lambda_2)_{R=B} = (\sigma_3\lambda_3)_{R=B}$$

$$= -P \equiv \frac{2G}{n}(1 - \lambda_a^{-2n}) \qquad (28)$$

Note that in eqs. (21) and (22), $\lambda_b \equiv 1$ and the integral is negligible.

Furthermore, the interior pancake stress is nearly hydrostatic, because

$$K + (4/3)G = K - (2/3)G \quad (\text{since } K \gg G)$$

This is the basis of the lubrication theory. Thus, one can carry out the spherical shell results to the interior of the pancake by assuming that each void is surrounded by its share of rubber matrix and by assuming, further, that the voids do not interact.

The interior field of the pancake extends to about $3a/4$. Beyond that, a boundary layer solution is in order.

In conclusion, it is hoped that this article stimulates other investigators to:

1. Measure pancake bulge and contraction.
2. Do all measurements at slow rates of displacements.
3. Do FEM calculations for large aspect ratios.
4. Characterize the rubber uniaxially and equibiaxially.
5. Measure the equibiaxial failure strain.

APPENDIX

We choose a right-handed coordinate frame (see sketch below):

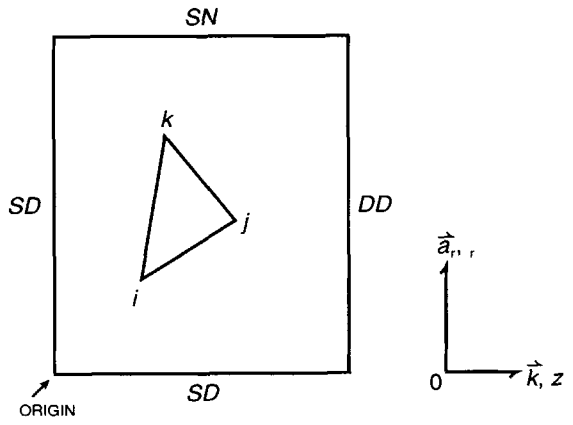

Somewhere in the domain of the quarter-pad, a triangle is embedded, whose vertices serve as nodes, lettered (i, j, k) in counterclockwise order, and which serve as an even transposition of the reference cycle (1, 2, 3). The vectors to the nodal points are denoted by r_i and the displacement vectors by u_1.

If one assumes u in the triangle is given by

$$\vec{u} = \vec{A} + \vec{B}z + \vec{C}r \qquad (A\text{-}1)$$

one evaluates u at (i, j, k) and inverts the matrix, then

$$\vec{u} = \frac{\sum_i \vec{u}_i(A_i + B_i z + C_i r)}{\sum_i A_i} \qquad (A\text{-}2)$$

where

$$A_i = e_{ijk} z_j r_k;\ 2 \times \text{area of triangle} = \sum_i A_i$$

$$B_i = e_{ijk} r_j 1_k$$

$$C_i = e_{ijk} 1_j z_k \quad \text{with} \quad d_j,\ k \text{ summed} \tag{A-3}$$

It follows that:

$$e_r = \frac{\sum_i u_i C_i}{\sum_i A_i}$$

$$e_\theta = \frac{1}{\sum_i A_i} \sum_i u_i \left(\frac{A_i + B_i z}{r} + C_i \right)$$

$$e_z = \frac{\sum_i w_i B_i}{\sum_i A_i}$$

and

$$e_{rz} = \frac{\sum_i (u_i B_i + w_i C_i)}{2 \sum_i A_i} \tag{A-4}$$

For triangle I,

$$\Phi = \int_0^{h/2} dz \int_0^{2az/h} 2\pi r\, dr W \tag{A-5}$$

For triangle II,

$$\Phi = \int_0^{h/2} dz \int_{2az/h}^{a} 2\pi r\, dr W \tag{A-6}$$

REFERENCES

1. C. C. Surland, *J. Appl. Polym. Sci.*, **11,** 1227 (1967).
2. P. J. Blatz, *Bulletin 2nd Meeting ICRPG Working Group on Mechanical Behavior,* CPIA Pub. No. 27, 1, October 1963.
3. W. T. Milloway, C. C. Surland, and I. Skulte, *JANAF-ARPA-NASA Panel on Physical Properties of Solid Propellants,* SPIA/PP14-0c, Vol. I, October 1961.
4. L. R. Herrmann, *Bulletin 2nd Meeting ICRPG Working Group on Mechanical Behavior,* CPIA, Pub. No. 27, 97, October 1963.
5. P. J. Blatz, *Rheology, Theory and Applications,* F. R. Eirich, Ed., Vol. 5, Academic, New York, London, 1969.
6. H. G. Kilian and H. Schenk, *J. Appl. Polym. Sci.* **35,** 345 (1988).
7. P. A. Kakavas, Ph.D. Dissertation, University of Southern California, 1987.
8. L. A. Wood, G. W. Bullman, and G. E. Decker, *J. Res. N.B.S.-A.,* **76A,** 1 (1972).
9. A. Lepie, reference can be provided by P. J. Blatz.
10. M. Levinson, Ph.D. Dissertation, California Institute of Technology, Pasadena, California, 1964.
11. C. H. Lindsey, R. A. Schapery, M. Williams, and A. Zak, Aerospace Research Laboratories Report ARH., 63–152, September 1963.
12. G. Pickett, *J. Appl. Mech.,* A176 (September 1944).
13. B. T. Brady, *Int. J. Rock Mech. Min. Sci.,* **8,** 165 (1971).
14. N. Warren, *J. Geophys. Res.,* **78**(2), 352 (1973).
15. R. W. Ogden, *Proc. Roy. Soc. London,* **A326,** 565 (1972).

Received October 30, 1991
Accepted February 1, 1993